The Use of Spatial Graphs for Optimal Obstacle Placement: A Study on Impact of the Clutter Spatial Distribution

Vural Aksakalli[a], Elvan Ceyhan[b]

[a]*Department of Industrial Engineering, Istanbul Şehir University, Istanbul 34662, Turkey*
[b]*Department of Mathematics, Koç University, Istanbul 34450, Turkey*

Abstract

Consider a situation where the goal is to place true obstacles in an environment cluttered with false obstacles in order to maximize the total traversal length of a navigating agent (NAVA). Prior to the traversal, NAVA is given location information and probabilistic estimates of each disk-shaped regions being a true obstacle. The NAVA can disambiguate a disk's status only when situated on its boundary. There exists an obstacle placing agent (OPA) that locates obstacles prior to NAVA's traversal. The goal of OPA is to place true obstacles in between the clutter in such a way that NAVA's traversal length is maximized in a game-theoretic sense. We call this the optimal obstacle placement with disambiguations problem. A particular variant we consider is the one where OPA knows the clutter spatial distribution type, but not the exact locations of clutter disks. In this study, we show how such a continuous obstacle field can be fruitfully discretized using spatial graphs. We discuss the impact of different clutter spatial distribution types on the optimal obstacle placement scheme including homogeneous and inhomogeneous Poisson, Matern, Thomas, Strauss and hardcore spatial distributions. Our methodology is based on utilization of repeated measures analysis of variance for analysis of traversal lengths for various obstacle placing schemes for identification of the optimal combination.

Keywords: Spatial graph, repeated measures analysis of variance, spatial point process, stochastic optimization

1. Introduction

The stochastic obstacle scene (SOS) problem is a challenging stochastic optimization problem that has practical applications in robotics, computer vision, and naval logistics. SOS Problem was first introduced by Papadimitriou and Yannakakis (1991), and its graph-theoretic version was called the *Canadian traveler's problem*. Both continuous and graph-theoretic versions of the problem are computationally intractable, and both versions have gained considerable attention recently (see, e.g., Nikolova and Karger (2008); Xu et al. (2009); Likhachev and Stentz (2009); Eyerich et al. (2009); Aksakalli et al. (2011)). In this article, we consider a slightly modified version of the original SOS problem. In this version, a point-sized navigating agent (NAVA) needs to quickly traverse from a given starting point to a target point through an arrangement of disk-shaped regions (these regions shall be referred to as "disks" henceforth for brevity). Some of these disks are true obstacles placed by another agent, called the *obstacle-placing agent* (*OPA*), and the rest is clutter, i.e., false obstacles. For instance, in case of a naval logistics application, the true obstacles would be mines, and the clutter could be rocks, metal pieces, debris, etc. The OPA places the true obstacles in between the clutter prior to NAVA's traversal. At the outset, the NAVA does not

Email addresses: aksakalli@sehir.edu.tr (Vural Aksakalli), elceyhan@ku.edu.tr (Elvan Ceyhan)

know the actual status of any disk. However, the NAVA is given respective probabilities of each disk being a true obstacle or a clutter. Over the course of the traversal, the NAVA has the option to disambiguate any (ambiguous) disk, i.e., learn with 100% accuracy if it is a true obstacle. This disambiguation can be performed when the NAVA is situated on a disk's boundary. The NAVA can pass through a disk only if a disambiguation reveals that it is clutter, i.e., not a true obstacle. We assume that there is no limit on the number of available disambiguations, and that disambiguations can be executed only at a cost added to the overall length of the traversal. We also assume that the obstacle scene is static, that is, the disks do not change location during the traversal, and the obstacle/clutter status of a disk never changes. The NAVA's challenge is to decide what and where to disambiguate en route so as to minimize the total length of the traversal. This problem is called the SOS problem. The OPA's challenge, on the other hand, is to place a given number of true obstacles in between the clutter so as to maximize the traversal length of the NAVA in a game-theoretic sense. We call this problem the *obstacle placement with disambiguations problem*, or the *OPD problem* in short.

Algorithms in the literature for the SOS problem and its variants— both in continuous and discrete settings—have assumed that the spatial distribution of possible-obstacles is given. In this work, which is partially based on the article Aksakalli and Ceyhan (2012), we consider a particular variant of the OPD problem where OPA knows the clutter spatial point distribution (called clutter type for brevity), but not the exact locations of the clutter disks. The motivation for this variant is that the clutter location information requires specific knowledge of the NAVA's sensor technology, which is not necessarily accessible to OPA. Nonetheless, it is still likely that OPA has information on the *spatial distribution* of the clutter disks. For instance, rock or debris distribution along a specific coastline might follow a certain spatial point distribution that is known to OPA. Our goal is to gain insight into which obstacle placement scheme works better for which clutter type, and explore the effect of the number of obstacles on NAVA's traversal length. In particular, we would like to address the following critical research question: Given a clutter type, what is the optimal placement scheme and the optimal number of obstacles that should be used?

The primary analysis tool we use is repeated measures analysis of variance (ANOVA). Our specific setup leads to a three-way repeated measures ANOVA problem where the treatment factors are as follows:

Clutter type: We consider 6 different point processes for sampling clutter disk centers: homogeneous and inhomogeneous Poisson processes, Matérn and Thomas clustered point processes, and hardcore and Strauss regular point processes.

Number of obstacles: We consider 5 different number of obstacles (20, 30, 40, 50, and 60, respectively).

Obstacle layout scheme: We experiment with a total of 19 different obstacle placement patterns. These patterns are sampled from a homogeneous Poisson process within four different window forms: the clutter sampling window itself, linear, V-, and W-shaped polygonal windows.

The response variable here is the total traversal length of the NAVA including the cost of disambiguations. Without loss of generality, we assume a fixed radius for both obstacle and clutter disks. For computational efficiency, we resort to spatial graphs. In particular, we work with an 8-adjacency integer lattice discretization of the continuous setting with diagonal edges as in Aksakalli et al. (2011). As for NAVA's navigation algorithm, we use a simple adaptation of the Reset Disambiguation Algorithm in Aksakalli et al. (2011) for the lattice discretization, which we call the *Adapted RD* (*ARD*) Algorithm. The reader is referred to Fishkind et al. (2007) for a review of the literature that includes the history and development of the problems that fall under the SOS problem umbrella.

In our computational experiments, the lattice used is $[1, 100] \times [1, 100]$, with $s = (50, 100)$ and $t = (50, 1)$. Each disk has a radius of 4.5 units, and the disk centers are sampled on the pairs of real numbers in $[10, 90] \times [10, 90]$—ensuring that there is always a permissible walk from s to t. The cost of disambiguation is taken as 5. As in Priebe et al. (2005), clutter marks are sampled from Beta(6,2) (with a mean of 0.25) and obstacle marks are sampled from Beta(2,6) (with a mean of 0.75). This particular setup has been specifically designed to possess similar characteristics to an actual U.S. Navy minefield data set, called the COBRA data, which was presented in Witherspoon et al. (1995) and later used in Fishkind et al. (2007), Ye and Priebe (2010), and Ye et al. (2011).

2. Clutter Point Distributions

Formally, a *spatial point process* X is a finite random subset of a bounded region $\Omega \subset \mathbb{R}^2$. A realization of this point process, on the other hand, is called a *spatial point pattern*. Classical literature on the subject mainly identifies three spatial point pattern categories based on the nature of inter-point interactions: (1) independent patterns, (2) cluster patterns where points tend to be close to one another, and (3) regular patterns where points tend to avoid each other (Baddeley, 2010). In this study, we consider two patterns from each one of these three categories in turn, and this section describes those six spatial point processes used to generate background clutter disk centers in the OPD problem. Classical treatments of general spatial point patterns can be found in Cressie (1993) and Rippley (2004).

2.1 Homogeneous and Inhomogeneous Poisson Processes

In the context of spatial point processes, intensity is the average density of points per unit area in the region over which the point process is defined. In general, the null model in a point pattern analysis is the *homogeneous Poisson point process* in the plane with constant intensity λ, which is also called *complete spatial randomness* (*CSR*). CSR with intensity λ will be denoted by $CSR(\lambda)$. For any finite region R, the CSR point process has four properties: (1) the number of points in R is a Poisson random variable, (2) number of points in any two disjoint regions R and R' are independent random variables, (3) the expected number of points in R is $\lambda \cdot \text{area}(R)$, and (4) points in R are independently and uniformly distributed.

In the OPD problem, a possible scenario is that the density of the clutter increases from the start point toward the target point or vice versa. For instance, the density of rocks and/or debris along a coast line might increase as one traverses towards the coast. To simulate such a scenario, we consider the *inhomogeneous Poisson process*. This process is a modification of CSR where the intensity is not constant, but varies from location to location. Specifically, the intensity is a function in two dimensional Euclidean space. Let $IP(\lambda(h))$ denote the inhomogeneous Poisson process with intensity $\lambda(h)$ where $h \in \mathbb{R}^2$. Here, the intensity function $\lambda(h)$ specifies the values of λ on the plane. Properties of $IP(\lambda(h))$ are the same as those of $CSR(\lambda)$ with the last two properties modified as follows: $(3')$ the expected number of points in R is $\int_R \lambda(h)dh$, and $(4')$ points in R are independently and identically distributed with probability density $f(h) = \lambda(h) \left[\int_R \lambda(h)dh\right]^{-1}$.

2.2 Matérn and Thomas Clustered Point Processes

In many real-world contexts, existence of a point at a specific location increases the probability of other points being located in its vicinity, giving rise to a *clustered point process*. Some examples include human settlements, plants, stars, galaxies, and molecules (Daley and Vere-Jones, 2002). In particular, it might be more realistic to model clutter type in the OPD problem, such as rock formation and debris dispersal along a coastline, as a clustered point process rather than CSR.

A commonly-encountered cluster point process model in the literature is the *doubly-stochastic Poisson process*, which is also known as the *Cox process*. This process is a generalization of the Poisson process where the intensity parameter is randomized (Daley and Vere-Jones, 2002). In this work, we consider two special cases of the Cox process: *Matérn* and *Thomas point processes*.

The Matérn point process, denoted $M(\lambda, \mu, r)$, is constructed by first generating a Poisson point process of "parent" points with intensity λ. Each parent point is then replaced by a random cluster of points where the number of points in each cluster is sampled from a Poisson distribution with parameter μ. These child points are placed independently and uniformly inside a disk with a fixed radius, r, centered at the parent point.

Similar to the Matérn point process, the Thomas process, denoted $T(\lambda, \mu, \sigma)$, is constructed by first generating a Poisson point process of "parent" points with intensity λ. A random cluster of points replaces each parent point with the number of points per cluster being sampled from a Poisson distribution with parameter μ. In contrast with the Matérn point process, positions of these child points in the Thomas point process are isotropic Gaussian displacements centered at the cluster parent location with standard deviation σ.

2.3 Hardcore and Strauss Regular Point Processes

Another potential scenario in the OPD problem is where there is a "regularity" to the clutter disks. That is, the clutter center points tend to be a certain distance away from the other clutter center points. We consider two regular spatial point patterns with pairwise interactions: the *hardcore* and *Strauss point processes*. The probability density function of the hardcore process is that of the Poisson process with intensity λ conditioned on the event that no two points generated by the process are closer than d units apart, hence denoted at $HC(\lambda, d)$. The Strauss process, denoted $S(\lambda, d, \gamma)$, on the other hand, generalizes the hardcore process by incorporating a $\gamma \in [0, 1]$ parameter that controls of the interaction between the points. The process exhibits more regularity for smaller values of γ, and less regularity for larger γ. For $\gamma = 0$, the Strauss process becomes a hardcore process, and for $\gamma = 1$, it reduces to CSR (Baddeley, 2010).

2.4 The Clutter Sampling Procedure

In our computational experiments, all spatial point processes—both clutter and obstacle—are simulated via the `spatstat` package in the R programming environment (Baddeley and Turner, 2005). This particular package assumes that the point processes extend throughout the two-dimensional Euclidean space, but they are observed inside a sampling window P. In our case, the sampling window for the clutter center points is taken as $P = [10, 90] \times [10, 90]$. In sampling of the inhomogeneous Poisson process, points are generated so that clutter density increases from the top of the obstacle field toward the bottom where the target is located. Specifically, the intensity function is taken as $\lambda(x, y) = 0.037e^{(10-y)/40}$ on the sampling window P, which results in 100 points on the average.

In sampling of the Matérn and Thomas point processes, we work with $M(10, 10, 10)$ and $T(10, 10, 5)$ respectively. As for the hardcore and Strauss processes, we sample from $HC(100, 5)$ and $S(100, 5, 0.5)$. We use the Metropolis-Hastings algorithm while sampling from the hardcore and Strauss processes which is essentially a Markov chain whose states are spatial point patterns and its limiting distribution is the desired point process. After running the algorithm for a large number of times, which is 100,000 iterations in our experiments, the state of the algorithm is considered to be a realization of the desired point process (Baddeley, 2010).

Parameter values of all the six clutter types are chosen such that the number of points in any sampled point realization would be roughly 100 on the average. For instance, CSR is sampled with number of points being Poisson(100), and the $h(x, y)$ function we use for the inhomogeneous

Poisson process results in 100 points on the average. However, the actual number of points in each clutter realization that we use in our experiments is taken to be exactly 100. This is achieved by rejection sampling, i.e., by discarding sampled realizations for which number of points is different than 100. The benefit of fixing the number of clutter disks is that variation in traversal lengths resulting from the different number of clutter disks is removed. Thus, the only source of variation in the background clutter in our computational experiments is the spatial distribution of these 100 clutter disks. Figure 1 illustrates sample realizations from the clutter point processes within our simulation environment.

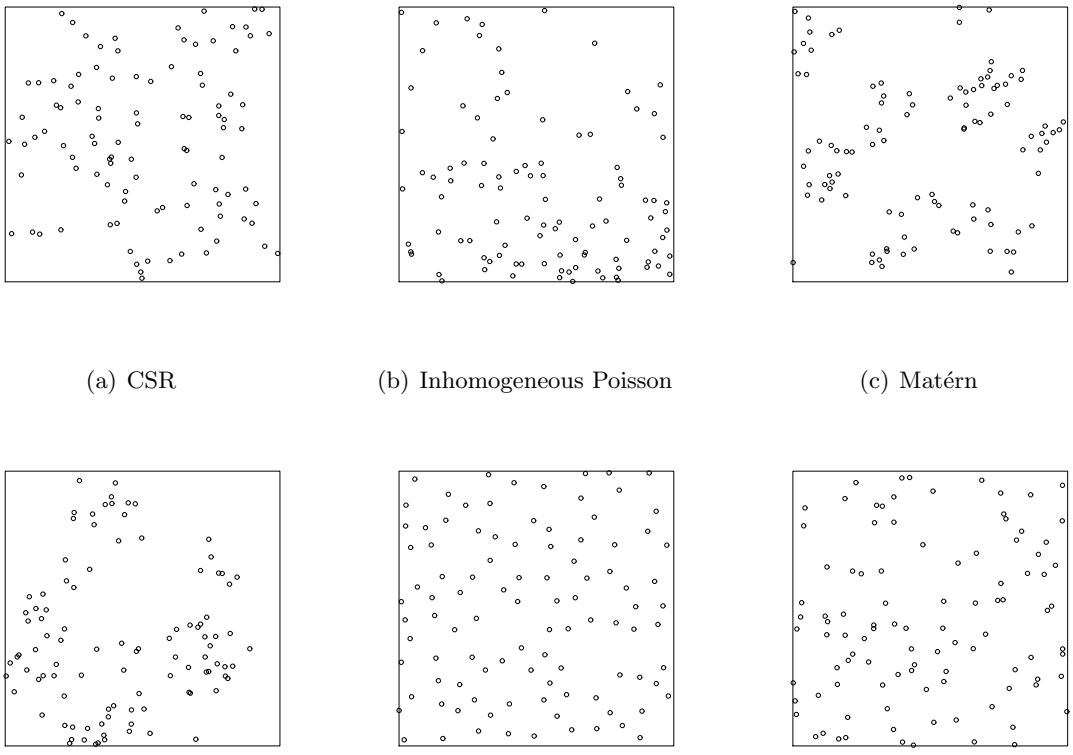

(a) CSR (b) Inhomogeneous Poisson (c) Matérn

(d) Thomas (e) Hardcore (f) Strauss

Figure 1: Sample realizations from the six background clutter spatial point distributions. The specific distribution parameters used are as follows: (a) $CSR(100)$, (b) $IP(0.037e^{(10-y)/40})$, (c) $M(10, 10, 10)$, (d) $T(10, 10, 5)$, (e) $HC(100, 5)$, and (f) $S(100, 5, 0.5)$. These parameters are chosen such that the number of points in any sampled point realization would be about 100 on the average. Rejection sampling was then utilized to have exactly 100 points in all the clutter realizations.

3. Obstacle Placement Schemes

As mentioned earlier, the goal of OPA is to place a certain number of true obstacles in the obstacle field under the assumption that OPA knows the spatial point distribution of the background clutter disks, but not their exact locations. On the other hand, the NAVA only has probabilistic information of each disk being a true obstacle. The NAVA, however, can distinguish true obstacles from the clutter only when situated at a disk's boundary. In this study, we limit our focus to CSR for sampling true obstacle disk centers within a total of 19 different sampling windows. One might

also consider inhomogeneous Poisson process for sampling the obstacle disk centers within these sampling windows. In fact, increasing the obstacle intensity along the $s - t$ line might perhaps increase NAVA's traversal length in general. However, we limit our focus to CSR for sampling the obstacle disk centers for the following reasons: First, OPA might not know the exact starting and target points of NAVA in practice. Second, the area in which OPA wishes to place obstacles might not be a square region as in our experiments, but perhaps an entire coastline. Thus, it makes more sense from an operational point of view to sample the true obstacle disk centers with uniform intensity inside their respective polygons.

We consider a total of 19 different sampling windows for the obstacle disk centers. The first sampling window is the polygon $P = [10, 90] \times [10, 90]$, i.e., the sampling window for the background clutter. For the remaining windows, we consider 80-unit long and 10-unit wide polygons as described below.

- 8 different linear windows with their top left corner y-coordinate being $90, 80, \ldots, 20$, and
- 5 different V-shaped and W-shaped windows, respectively, with their top left corner y-coordinate being $90, 80, \ldots, 50$. Difference between the top and bottom y-coordinates of each one of these 10 polygons is taken as 50 units.

The obstacle sampling window coinciding with the background clutter window itself is code-named as P. Other sampling windows are code-named by the polygon type ("L", "V", or "W" respectively) followed by the top left corner coordinate of the polygon. These 4 polygon shapes will be referred to as *obstacle forms*.

For example, L70 is the polygon whose four corner points are (10,70), (90,70), (90,60), and (10,60) clock-wise starting with the top left corner. The polygon V70's six corner points are (10,70), (50,40), (90,70), (90,60), (50,30), and (10,60); again clock-wise starting with the top left corner. Similarly, polygon W70's ten corner points are (10,70), (30,40), (50,70), (70,40), (90,70), (90,60), (70,30), (50,60), (30,30), and (10,60). The polygon W50, for instance, is the same as W70 shifted down 20 units along the y-axis. Thus, the 19 obstacle sampling windows we consider are P, L90, L80,...,L20, V90, V80, ...,V50, and W90, W80, ...,W50. The reason we consider the same polygon shape placed at different y-coordinates is that we are not only interested in which polygon shape is more efficient (in terms of increasing NAVA's total traversal length), but also which y-coordinate (i.e., distance to the target) is more efficient for a given polygon shape. We do not consider placing true obstacles along a straight horizontal line, as detection of such obstacle patterns by the NAVA would be relatively straightforward—see, e.g., Muise and Smith (1995) and Walsh and Raftery (2002) for detecting obstacles laid in such linear patterns.

In order to assess the impact of the number of true obstacles in the OPD problem, we consider five different number of obstacles for each one of the 19 obstacle sampling windows: 20, 30, 40, 50, and 60. As mentioned earlier, CSR conditioned on a specific number of points is in fact a uniform distribution with that many points. Therefore, the obstacles we consider are essentially uniformly distributed inside their respective sampling windows. Realizations of obstacle patterns are denoted by the sampling window followed by the number of obstacles. For instance, P:40 and L70:40 refer to the obstacle patterns sampled within the P and L70 windows, respectively, with 40 obstacle center points inside their respective windows.

4. Experimental Setup and the Statistical Analysis

Our particular experimental setup leads to a three-way ANOVA problem. The treatment factors are the background clutter type, the obstacle placement window, and the number of obstacles. The response variable is NAVA's total traversal length from s to t. The first treatment factor has 6 levels,

the second has 19, and the third has 5 levels, resulting in a total of 570 treatment combinations. Our primary goal here is to investigate whether there are any (statistically significant) differences between traversal lengths of different obstacle placement windows for a given number of obstacles and a given clutter type.

For each one of these 570 treatment combinations, we ran 100 Monte Carlo simulations. Each simulation consists of generating the obstacle field (i.e., the obstacle pattern superimposed on a clutter pattern) and, executing the ARD algorithm to find the shortest $s-t$ walk. The runtime per simulation averaged over the 57000 simulations was 9.5 seconds on a personal computer with an Intel Core i7 processor with 2.8 gigahertz clock speed.

As discussed earlier, each background clutter realization is sampled to have exactly 100 clutter disks via rejection sampling. In order to exclude the source of variability due to different clutter realizations for a given clutter type, we adopted a repeated measures approach in our experiments. That is, we sampled only 100 clutter realizations from each one of the 6 clutter types corresponding to each one of the 100 simulations for a given treatment combination. Thus, a total of 600 clutter patterns were generated for our experiments. For instance, the same CSR clutter realization was used for all of the 95 obstacle pattern-obstacle number combinations (19 obstacle patterns and 5 obstacle number levels) for the first Monte Carlo simulation. For the second Monte Carlo simulation, a different CSR realization was sampled and this realization was used for all of the 95 obstacle pattern-obstacle number combinations, and so on.

4.1 Repeated Measures ANOVA

The background clutter types (abbreviations presented in parentheses) we consider are Complete Spatial Randomness (CSR), inhomogeneous Poisson (IP) distribution, Matérn (M) distribution, Thomas (T) distribution, hardcore (HC) distribution, and Strauss (S) distribution. For convenience in presentation, the obstacle types are sometimes numbered from 1 to 19, or labeled in a more descriptive fashion such as V90 which stands for V-shaped obstacle window whose top left corner y-coordinate is 90. The 19 obstacle placement window types are sampled within 4 different polygon shapes (short notations are provided in parentheses): the entire P window (P), linear windows (L), V-shaped windows (V), and W-shaped windows (W). The obstacle window numbering of 1 to 19 corresponds to P, L90, L80, ..., L20, V90, V80, ..., V50, W90, W80, ..., W50, respectively. The obstacle number levels are $20, 30, \ldots, 60$. As mentioned earlier, for precision in our analysis, we used the same background clutter realization for each of the 95 obstacle type and obstacle number combination. Thus, we denote the traversal length as T_{ijkl} which is the traversal length of the measurement l for clutter type i, obstacle window type j, obstacle number level k with $l = 1, 2, \ldots, 100$, $i = 1, 2, \ldots, 6$, $j = 1, 2, \ldots, 19$, and $k = 1, 2, \ldots, 5$, respectively. Clutter types $1, 2, \ldots, 6$ correspond to CSR, IP, M, T, HC, and S patterns, respectively, and obstacle number levels $1, 2, \ldots, 5$ correspond to $20, 30, \ldots, 60$, respectively. Note that T_{ijkl}, $T_{ij'kl}$, $T_{ijk'l}$, $T_{ij'k'l}$ are measured on the same realization of the clutter type i, hence these measures are potentially correlated. In particular, the measurements on consecutive obstacle number levels (with other factors being same), would be highly (and perhaps positively) correlated. A similar trend can be expected for measurements within each type of obstacle window types (such as linear, V-shaped, or W-shaped obstacle forms) as a function of the distance to the target (i.e., as a function of the magnitude of the y coordinate). To take such correlation structure into account, we use *repeated measures ANOVA* techniques in our analysis to compare the traversal length differences between treatment factors, and possibly existence or lack of any interaction between these factors.

4.2 Comparison of Best Performers at Each Clutter Type

From OPA's perspective, it is more desirable to make the NAVA traverse longer lengths to reach the target point. Furthermore, in our scenario OPA is assumed to have no control on the

clutter type, but can only determine/know the clutter type (but not the actual locations of the clutter disks). Hence, for a given background clutter type, it is desirable to determine the obstacle type-obstacle number combination that yields the longest traversal lengths. This combination is referred to as "best performer" henceforth. The overall best performer and best performers for each obstacle type at each clutter type are presented in Table 1.

CSR Clutter					
obs. form	Overall	P	**Linear**	**V-Shaped**	W-Shaped*
trt comb.	V80:50	P:60	L20:50	V80:50, V50:40, V70:50	W50:60, W50:50
mean length	—	154.36	175.93	178.93	172.22
Inhomogeneous Poisson Clutter					
obs. form	Overall	P	Linear	**V-Shaped**	W-Shaped
trt comb.	V90:60	P:60	L20:40	V90:60	W90:60
mean length	—	155.46	170.40	188.96	173.60
Matérn Clutter					
obs. form	Overall	P	Linear	**V-Shaped**	W-Shaped
trt comb.	V90:50	P:60	L20:40	V90:50	W90:60
mean length	—	150.59	173.23	184.39	171.21
Thomas Clutter					
obs. form	Overall	P	**Linear**	**V-Shaped**	**W-Shaped**
trt comb.	V90:60	P:60	L20:50	V90:60	W60:60
mean length	—	143.09	176.15	181.48	177.56
Hardcore Clutter					
obs. form	Overall	P	Linear	**V-Shaped**	W-Shaped
trt comb.	V90:50	P:60	L20:40	V90:50	W80:60, W50:60
mean length	—	163.86	174.43	190.29	177.04
Strauss Clutter					
obs. form	Overall	P	Linear*	**V-Shaped**	W-Shaped
trt comb.	V80:40	P:60	L20:40	V80:40, V90:50	W80:60, W50:60
mean length	—	158.94	179.45	188.56	177.56

Table 1: The best performers (i.e., the obstacle type-obstacle number combination with the longest traversal lengths) for each background clutter type and the corresponding average traversal lengths. The best performer row is labeled as "trt comb.", and obstacle form as "obs. form". The "Overall" column is the best performer treatment combination at each clutter type. The obstacle type with the largest traversal lengths (that are significantly larger than the rest at 0.01 level) are marked in bold face, and the traversal lengths that are not significantly different at 0.05 level but different at 0.10 level are marked with an asterisk *.

Since there are multiple best performer obstacle type-obstacle number combinations at some clutter types (see Table 1), we compare the traversal lengths of best performers for obstacle form levels at each clutter type. At each background clutter type, we consider the following model with four different var-cov structures:

$$T_{ij} = \mu_0 + \mu_i^{OF} + \varepsilon_{ij} \tag{1}$$

where μ_0 is the overall mean, μ_i^{OF} is the main effect of obstacle form i, and ε_{ij} is the error term for $i = 1, 2, 3, 4$ (which correspond to P, linear, V-shaped, and W-shaped obstacle forms) and $j = 1, 2, \ldots, n_i$ where n_i is $k \times 100$ with k being the number of treatment combinations that are best performers. For example for the CSR clutter type, $k = 1$ for P obstacle type and $k = 3$ for the V-shaped obstacle type. The var-cov structures we consider are compound symmetry (CS), unstructured (UN), autoregressive var-cov structure (AR1), autoregressive heterogeneous (ARH1).

When Mauchly's test is performed, we obtain $p < 0.0001$ for the CSR clutter, $p = 0.2172$ for the inhomogeneous Poisson clutter, $p = 0.1032$ for the Matérn clutter, $p = 0.0005$ for the Thomas clutter, $p = 0.0764$ for the hardcore clutter, and $p = 0.0002$ for the Strauss clutter. That is, for inhomogeneous Poisson clutter, we can assume CS in var-cov structure, and for Matérn and hardcore clutters, it is a close call for being significant, so we also consider the AIC values and likelihood ratio p-values which are presented in Table 2. Notice that at inhomogeneous Poisson clutter the model with CS var-cov structure (which agrees with the result of Mauchly's test), and at other clutter types the model with ARH1 var-cov structure seem to be the best model, since these models have the smallest AIC values. The p-values are based on the likelihood ratio of the model with smallest AIC and the model in the corresponding row. Hence, when Mauchly's test yields an almost significant p-value, we also consider the model selection criteria such as AIC and log likelihood measures. If the likelihood ratio test is not significant for two models, we follow the common practice of picking the simpler model (i.e., the model with fewer parameters). With the best models, we observe significant differences between obstacle types.

The longest traversal lengths (that are significantly larger than the others) at each clutter type among the best performers are marked in bold face in Table 1. For each clutter type, we compare the mean traversal lengths of the best performer obstacle type-obstacle number combinations by Tukey's HSD (honestly significant difference) method on mean differences (Miller (1981)). Best performers for each clutter type are described below.

CSR Clutter: The longest lengths (that are significantly larger than others) among best performers (in decreasing order) are at V-shaped, linear, and W-shaped obstacle forms. That is, the lengths for the V-shaped, linear, and W-shaped best performers are not significantly different from each other at 0.05 level, although for the mean difference between V-shaped and W-shaped best performers have p-value 0.0645. Hence for the CSR clutter, we recommend the use of V80:50, V50:40, V70:50 or L20:50 obstacle type in this order. That is, if the cost of the above obstacle placements is about the same, then any one of them can be used but V80:50 has a slight advantage, otherwise the one with the lowest cost is recommended.

Inhomogeneous Poisson Clutter: The longest length among best performers is at V-shaped obstacle forms. Hence V90:60 obstacle type is recommended.

Matérn Clutter: The longest length among best performers is at V-shaped obstacle forms. Hence V90:50 obstacle type is recommended.

Thomas Clutter: The longest lengths among best performers (in decreasing order) are at V-shaped, W-shaped, and linear obstacle forms. That is, the lengths for the V-shaped, W-shaped, and linear best performers are not significantly different from each other at 0.05 level. Hence V90:60, W60:60, or L20:50 obstacle types are recommended in this order. If there are no cost restrictions, V90:60 has a slight advantage, otherwise the one with cheapest construction can be employed.

Hardcore Clutter: The longest length among best performers is at V-shaped obstacle forms. Hence V90:50 obstacle type is recommended.

Strauss Clutter: The longest lengths among best performers (in decreasing order) are at V-shaped and linear obstacle forms, although for the mean difference between V-shaped and linear best performers have p-value 0.0745. Hence V80:40 or V90:50 obstacle types are recommended in this order as in the previously discussed sense.

CSR Clutter Type					
var-cov structure	df	AIC	-log likelihood	L-ratio	p-value
CS	6	7490.54	3739.27	101.98	$< .0001$
UN	29	7421.18	3681.59	13.37	0.8608
AR1	6	7487.76	3737.88	99.21	$< .0001$
ARH1	9	7394.55	3688.28	—	—
Inhomogeneous Poisson Clutter Type					
CS	6	4048.91	2018.45	29.23	$< .0001$
UN	14	4028.11	2000.05	7.57	0.1815
AR1	6	4053.76	2020.88	34.08	$< .0001$
ARH1	9	4025.68	2003.84	—	—
Matérn Clutter Type					
CS	6	4159.92	2073.96	11.68	0.0086
UN	14	4162.26	2067.13	1.97	0.8536
AR1	6	4158.47	2073.24	10.24	0.0166
ARH1	9	4154.23	2068.12	—	—
Thomas Clutter Type					
CS	6	4197.73	2092.86	42.57	$< .0001$
UN	14	4167.06	2068.03	7.10	0.2136
AR1	6	4197.64	2092.82	42.48	$< .0001$
ARH1	9	4161.16	2071.58	—	—
Hardcore Clutter Type					
CS	6	5244.09	2616.04	42.63	$< .0001$
UN	14	5225.46	2594.73	—	—
AR1	6	5246.43	2617.21	44.97	$< .0001$
ARH1	9	5228.94	2605.47	21.47	0.0107
Strauss Clutter Type					
CS	6	6399.31	3193.66	66.04	$< .0001$
UN	23	6353.29	3153.65	13.97	0.4519
AR1	6	6398.92	3193.46	65.66	$< .0001$
ARH1	9	6339.26	3160.63	—	—

Table 2: The comparisons of the models for the best performer treatment combinations as in Equation (1) for each background clutter type. The column labels are degrees of freedom (df), Akaike information criterion (AIC), negative log likelihood value, likelihood ratio test (L-ratio). The models are with compound symmetry (CS), autoregressive (AR1), autoregressive heterogeneous (ARH1), and unstructured (UN) var-cov structure. The likelihood ratio (L-ratio) and the associated p-value are with respect to the model with the smallest AIC value.

5. Discussion and Conclusions

In this work, we consider the obstacle placement with disambiguations (OPD) problem wherein the objective is to place a given number of true obstacles in between the clutter so as to maximize the traversal length of the navigating agent (NAVA) in a game-theoretic sense. We consider a specific version of the problem where obstacle placing agent (OPA) knows the clutter type (i.e., the clutter spatial distribution), but not the exact location of clutter disks. We investigate relative efficiency of a variety of obstacle placement patterns against different background clutter types. Our goal is to explore the effect of the number of obstacles on NAVA's traversal length and to determine which obstacle placement patterns perform better for a given clutter type. We believe that such an analysis within a maritime minefield context has a significant potential in design of more efficient and cost-effective interdiction systems.

Acknowledgments

The work of V. Aksakalli was supported by The Scientific and Technological Research Council of Turkey (TUBITAK), Grant No. 111M541.

References

Aksakalli, V., Ceyhan, E., 2012. Optimal obstacle placement with disambiguations. Annals of Applied Statistics 6, 1730–1774.

Aksakalli, V., Fishkind, D., Priebe, C., Ye, X., 2011. The reset disambiguation policy for navigating stochastic obstacle fields. Naval Research Logistics 58, 389–399.

Baddeley, A., 2010. Analysing spatial point patterns in R. Workshop Notes Ver.4.1.

Baddeley, A., Turner, R., 2005. Spatstat: An R package for analyzing spatial point patterns. Journal of Statistical Software 12, 1–42.

Cressie, N., 1993. Statistics for spatial data. Wiley-Interscience, Hoboken, NJ.

Daley, D., Vere-Jones, D., 2002. An introduction to the theory of point processes, second ed. Edition. Springer, NY.

Eyerich, P., Keller, T., Helmert, M., 2009. High-quality policies for the Canadian travelers problem. Proceedings of the 24th AAAI Conference on Artificial Intelligence, Atlanta, Georgia.

Fishkind, D., Priebe, C., Giles, K., Smith, L., Aksakalli, V., 2007. Disambiguation protocols based on risk simulation. IEEE Transactions on Systems, Man, and Cybernetics, Part A 37 (5), 814–823.

Likhachev, M., Stentz, A., 2009. Probabilistic planning with clear preferences on missing information. Artificial Intelligence 173, 696–721.

Miller, R., 1981. Simultaneous Statistical Inference. Springer, NY.

Muise, R. R., Smith, C. M., 1995. A linear density algorithm for patterned minefield detection. Proceedings of the SPIE 2496, 586–593.

Nikolova, E., Karger, D. R., 2008. Route planning under uncertainty: the Canadian traveller problem. Proceedings of the 23rd AAAI Conference on Artificial Intelligence, Chicago, Illinois.

Papadimitriou, C., Yannakakis, M., 1991. Shortest paths without a map. Theoretical Computer Science 84, 127–150.

Priebe, C., Fishkind, D., Abrams, L., Piatko, C., 2005. Random disambiguation paths for traversing a mapped hazard field. Naval Research Logistics 52, 285–292.

Rippley, B., 2004. Spatial statistics. Wiley-Interscience, Hoboken, NJ.

Walsh, D. C., Raftery, A. E., 2002. Detecting mines in minefields with linear characteristics. Technometrics 44 (1), 34–44.

Witherspoon, N., Holloway, J., Davis, K., Miller, R., Dubey, A., 1995. The coastal battlefield reconnaissance and analysis (COBRA) program for minefield detection. Proceedings of the SPIE 2496, 500–508.

Xu, Y., Hu, M., Su, B., Zhu, B., Zhu, Z., 2009. The Canadian traveller problem and its competitive analysis. Journal of Combinatorial Optimization 18, 195–205.

Ye, X., Fishkind, D., Priebe, C., 2011. Sensor information monotonicity in disambiguation protocols. Journal of the Operational Research Society 62 (1), 142–151.

Ye, X., Priebe, C., 2010. A graph-search based navigation algorithm for traversing a potentially hazardous area with disambiguation. International Journal of Operations Research and Information Systems 1 (3), 14–27.